

DIVISION OF BRAIN CIRCUITS †



Professor
MATSUZAKI, Masanori

Assistant Professor:	HIRA, Riichiro MASAMIZU, Yoshito
Technical Staff:	OHSAWA, Sonoko
NIBB Research Fellow:	EBINA, Tepei
Postdoctoral Fellow:	TANAKA, Yasuhiro TANAKA, Yasuyo KONDO, Masashi SHINOTSUKA, Takanori TAKEDA, Yuta
SOKENDAI Graduate Student:	OHKUBO, Fuki HASEGAWA, Ryota SUZUKI, Ayami
Visiting Graduate Student:	TERADA, Shin-Ichiro
Visiting Scientist:	HIRAKAWA, Reiko
Technical Assistant:	HIMENO, Miki SAITO, Junko ATSUMI, Urumi OHARA, Kaori KOTANI, Keiko TAKAHASHI, Yoichi IWASE, Etsuko IMOTO, Eiko SUGIURA, Haruka
Secretary:	SUGIYAMA, Tomomi

Various firing patterns of many cortical neurons represent information processing in the brain. The microarchitecture of synaptic connections control information processing in cortical circuits. The structure and location of synapses determine and modify the strength of this information processing. The aim of our laboratory is to reveal how information is formed, maintained, selected, and decoded in the brain at the levels of single cells and of single synapses. To do so, we mainly use two-photon microscopy that allows us to see fluorescence signals from deep within living tissue, developing novel photostimulation methods and animal behavioral tasks. The goals of our recent studies are to reveal how voluntary movement is memorized and represented in cortical circuits. In addition, we are working to apply two-photon microscopy to non-human primates in order to understand information processing in the brain, which is relevant to high cognitive functions.

I. Cortical modules for discrete & rhythmic movements (Hira et al., J Neurosci., 2015).

Animal behavior has discrete and rhythmic components, such as reaching and locomotion. It is unclear how these movements with distinct dynamics are represented in the cerebral cortex.

We examined the dynamics of complex movements of freely movable forelimbs in awake ChR2 transgenic mice with the skull coated by transparent resin (Hira et al., 2009). The left cortical surface was illuminated by a blue laser (500-ms train of 2- or 4-ms duration pulses delivered at 50 Hz) focused through the objective lens (Fig. 1). We call this method pTOS. The pTOS-induced trajectory of the right forepaw was tracked in three-dimensional space by two high-

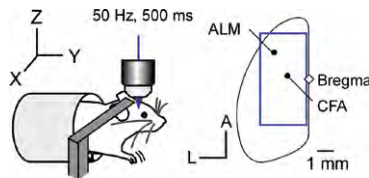


Figure 1. pTOS of an awake, head-restrained, ChR2 mouse. Right, the dorsal view of the left cerebral cortex. The blue square indicates the mapped area.

speed cameras at 100 or 200 frames/s.

pTOS induced one of two major types of right forelimb movement. During pTOS of the anterior lateral part of the motor cortex (ALM; Fig. 1), the right forepaw moved to a narrow space in every trial. By contrast, during pTOS of the caudal forelimb motor area (CFA; Fig. 1), the right forepaw moved circularly for more than one cycle and its end point varied. We categorize the former right-forelimb movement as a discrete movement, and the latter as a rhythmic movement. To map the representation of the discrete and rhythmic forelimb movements, we divided a 6×3 mm area of the left dorsal cerebral cortex into 16×8 sites (inter-site distance of $400 \mu\text{m}$) and performed pTOS at each site (Fig. 1). For the first analysis, the direction and distance from the mean initial point to the mean end point of the forepaw were calculated for each pTOS site. The direction and distance had clear topography in the cortex (arrows in Fig. 2). Long arrows on the map indicate the sites that induced forelimb movements with a limited target space and long distance. The ALM and the hindlimb motor area (HA), which is caudal to the CFA, had long arrows with almost opposite directions.

For each pTOS site, the tangential velocity profile of the averaged movement was fitted with a Gaussian function and the coefficient of determination was defined as the ‘discreteness index’. The domains with a large discreteness index (magenta in Fig. 2) corresponded to the ALM and the HA, which is consistent with the finding that these areas had long arrows on the map showing the direction and distance of the pTOS-induced movement (green in Fig. 2). We found that rhythmic movement with forward rotation was represented by the domain spanning from the medial part of the RFA to the CFA. The domain to induce the rhythmic movement was sandwiched by two domains to induce the discrete movements in forward and backward directions (forward discrete movement and backward discrete movement) (Fig. 2). When the photostimulation frequency was optimal, the time to reach maximum tangential velocity in the discrete movement was 136 ± 43 ms ($n=4$ mice) and the frequency with the maximum power of the rhythmic movement was 8.7 ± 0.28 Hz ($n=3$ mice). Thus, low-frequency photostimulation of the ALM generated a discrete movement with an intrinsic bell-shaped velocity profile, whereas high-frequency photo-

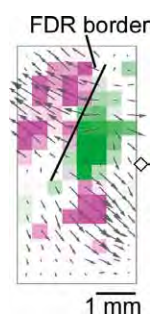


Figure 2. Maps of the discreteness index (magenta) and the rhythmicity index (green) overlain on the map of the direction and distance of the forelimb movement (arrows). The solid line indicates the FDR border.

†: This laboratory was closed on 31 March, 2016.

stimulation of the CFA generated a rhythmic movement with a relatively stable, intrinsic resonance property.

To determine whether the cortical domains to induce the discrete and rhythmic movements were hierarchical or parallel, we applied a mixture of AMPA/kainate receptor antagonist and NMDA receptor antagonist to the cerebral cortex. The size of the movement induced by pTOS of the ALM or CFA was not significantly reduced after the application of the blockers to the photostimulated areas. In addition, unsupervised clustering of the sites with cortico-cortical synaptic interactions obtained by the Allen Mouse Brain Connectivity Atlas (Oh et al., 2014) showed that the border

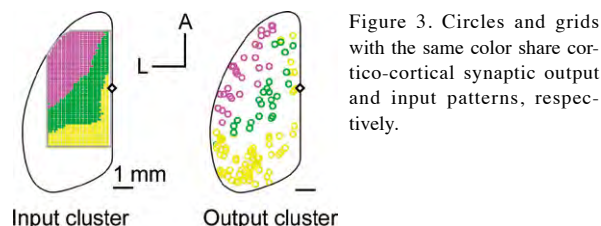


Figure 3. Circles and grids with the same color share cortico-cortical synaptic output and input patterns, respectively.

separating the two different clusters in the frontal cortex roughly corresponded to the FDR border (Fig. 3). Thus, the domains to induce the forward discrete movement and the rhythmic movement were functionally and anatomically distinct. We call such domains ‘modules’.

Photostimulation of either of the CFA or ALM suppressed spontaneous activity at the other site. The distance of the discrete movement induced by the simultaneous pTOS of the CFA and ALM was significantly shorter than that induced by pTOS of the ALM alone. Likewise, the power of the rhythmic movement was significantly smaller than that induced by pTOS of the CFA alone. Thus, the two distinct modules possess the ability to mutually weaken the neuronal activity and the movement induction elicited by the other module.

II. Cortical representation of ethologically relevant movements and lever-push/pull movements (Hira et al., J Neurosci., 2015).

Discrete and rhythmic movements might be a part of coordinated movements that involve multiple parts of the body. We extracted three types of ethologically relevant movements by detecting movements of other parts of the body as well as the right forelimb. These were termed ‘forepaw-to-mouth’, ‘defensive-like’, and ‘locomotion-like’ movements. Forepaw-to-mouth and locomotion-like movements were mainly elicited by pTOS of the ALM and the CFA, respectively. Defensive-like movement was induced by pTOS of the anterior and middle parts of the rhythmic module. The border between forepaw-to-mouth and defensive-like movements was almost identical to the FDR border. These results are consistent with the observation that the forepaw-to-mouth movement had a constant goal position and that defensive- and locomotion-like movements included oscillatory components.

Although the medial part of the RFA and the CFA were involved in the rhythmic module, neuronal activity in these areas is strongly related to a voluntary lever-pull movement that is not rhythmic (Hira et al., 2013; Masamizu et al.,

2014). Therefore, these areas may not function only for rhythmic movement. To assess this possibility, we conducted pTOS when a lever was located near the right forepaw in four mice.

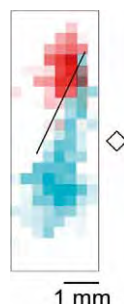


Figure 4. Maps of lever-push (red) and lever-pull (cyan) movements induced by pTOS. The solid line indicates the FDR border.

This stimulation exclusively induced a lever-push movement (red in Fig. 4). On the other hand, pTOS of the CFA preferentially induced a lever-pull movement (cyan in Fig. 4), which was sometimes followed by the rhythmic movement. The medial part of the RFA and the HA almost exclusively induced a lever-pull movement. The border of the lever-push and lever-pull movements roughly corresponded to the FDR border (Fig. 4). These results indicate that the distinct cortical modules adapted to distinct lever movements, and that the module for the rhythmic movement could induce a non-rhythmic movement.

Our results indicate that motor cortical neurons may not exclusively encode unique purposes or specific complex movements. Instead, a population of neurons in a motor cortical area may evolve to encode various purposeful movements depending on the environmental constraints and intrinsic dynamics.

III. Long-term two-photon calcium imaging of neuronal populations with subcellular resolution in adult non-human primates (Sadakane et al., Cell Rep., 2015).

We developed a new method for long-term imaging of a genetically encoded calcium indicator (GECI), GCaMP6f, expressed from adeno-associated virus (AAV) vectors in cortical neurons of the adult common marmoset (*Callithrix jacchus*), a small New World primate. We first cloned two components of the TET-Off system, namely, the tetracycline-controlled transactivator (tTA) under the control of the Thy1S promoter and GCaMP6f under the control of the tetracycline response element (TRE3) promoter, into separate AAV vectors (Fig. 5).

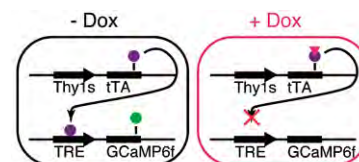


Figure 5. Schematic illustration of the TET-Off gene expression system.

In the absence of Dox, tTA constitutively activates expression of a transgene under the TRE3 promoter. Dox prevents the binding of the tTA to the TRE3, and inhibits transgene expression (Fig. 5).

For fluorescence imaging after AAV injection to the marmoset neocortex, marmosets were placed under the

microscope and lightly anesthetized by isoflurane inhalation. We detected strong epifluorescence signals around the injection site through the imaging window after only 10 days of AAV injection (Fig. 6). In many neurons, spontaneous calcium transients were clearly detected (Fig. 6).

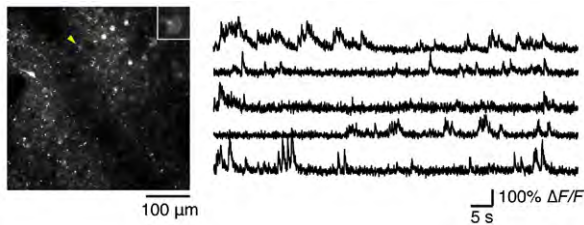


Figure 6. Left, representative two-photon image of GCaMP6f on post injection day 10. Right, representative $\Delta F/F$ traces from five ROIs in the field shown in left.

To test the effectiveness of Dox control in marmosets injected with AAV-TET-Off vectors, we administered Dox in drinking water to the animals for several days, and examined an image of the same area repeatedly over time. Twenty eight days after the start of the 5-day Dox administration, we were able to identify the same population of neurons that we observed before Dox administration. Spontaneous calcium transients were detected from the same neuron both before and after Dox administration. We observed a set of neurons with very similar configurations at an interval of more than 100 days after three trials of Dox administration, which are most likely to represent identical neuronal populations (Fig. 7).

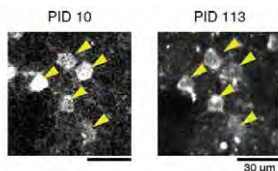


Figure 7. Representative images of GCaMP6f fluorescent signals on post injection days 10 and 118 from the same field.

Due to a high signal-to-noise ratio of the fluorescence signals, we were able to monitor the activity of neuronal somata located up to 400 μm from the cortical surface. This depth range is supposed to cover L1 and L2, as well as the upper part of layer 3 (L3). Using a piezoelectric objective mount, we continuously recorded the activity of multiple neurons with single-cell resolution from a relatively broad area (625 × 625 μm) at three depths: 150 μm, 275 μm, and 400 μm (from L2 to L3). In this experiment, 445 putative neuronal somata were determined and 81 of them were spontaneously active neurons.

Next, we tested whether neuronal responses evoked by tactile stimulation could be detected in the somatosensory cortex. For tactile stimulation, we attached vibrators to the arm and leg of marmoset B that were contralateral to the hemisphere with the imaging window, and stimulated each body part alternately for 1 s with an interval of 7.5 s. We found some neurons that responded to the tactile stimulation. Figure 8A shows two examples of neuronal soma in L3 whose fluorescence changes were clearly time-locked to the stimuli.

Consistent with the existence of stimulus-selective neurons, we also observed stimulus-selective responses from dendrites in L1 (Figure 8B) and axonal boutons in L1 (Figure 8C). The responses of these dendrites and axons to each stimulus were as robust as those of the somata.

Thus, our results demonstrate that the spatial and temporal profile of each neuron, dendrite, and axon in the marmoset cerebral cortex can be correlated with a variety of sensory stimuli. Our new technique removes a major obstacle to studying the non-human primate cortex using calcium imaging. In future studies, the technique, combined with various cognitive tasks, should shed light on the organization and plasticity of the primate cerebral cortex.

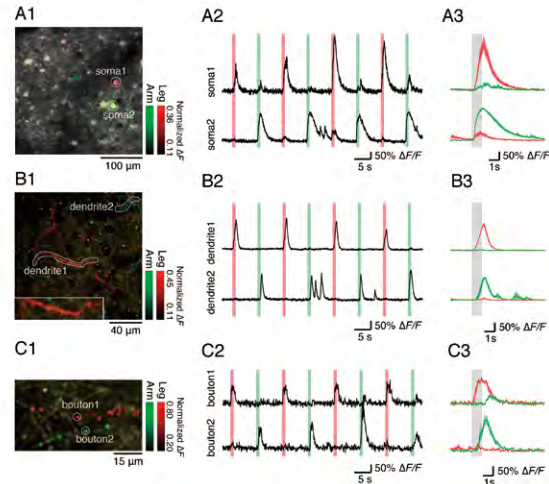


Figure 8. Selective sensory responses to tactile stimulation from neuronal somata (A), dendrites (B), and axonal boutons (C). Middle (2), the green and red lines indicate the timing of tactile stimulation to the left arm and the left leg, respectively. Right (3), the responses to nine stimuli to each body part were averaged. The gray band indicates the timing of the left arm and the left leg stimulation.

Publication List:

(Original papers)

- Hira, R., Terada, S., Kondo, M., and Matsuzaki, M. (2015). Distinct functional modules for discrete and rhythmic forelimb movements in the mouse motor cortex. *J. Neurosci.* 35, 13311-13322.
- Sadakane, O., Masamizu, Y., Watakabe, A., Terada, S., Ohtsuka, M., Takaji, M., Mizukami, H., Ozawa, K., Kawasaki, H., Matsuzaki, M., and Yamamori, T. (2015). Long-term two-photon calcium imaging of neuronal populations with subcellular resolution in adult non-human primates. *Cell Rep.* 13, 1989-1999.